A Stable Pillared-layer Metal-organic Framework for Recovery of C2H6 and C3H8 from Natural Gas

Yufang Wu[1], Zewei Liu[1], Xun Wang[1], and Zhong Li[1]

[1]South China University of Technology

May 29, 2020

Abstract

Separation and recovery of C2H6 and C3H8 from natural gas is a potentially economical but challenging subject in the petroleum industry. In this work, we report a stable pillared-layer microporous MOF, Ni(TMBDC)(DABCO)0.5 for the separation of C2H6 and C3H8 from natural gas. Ni(TMBDC)(DABCO)0.5 remained intact structure after exposure to humid air with RH = 100% for days. Derived from the combination of dense and accessible methyl group and methylene group in the channel, Ni(TMBDC)(DABCO)0.5 exhibited strong affinity toward C3H8 and C2H6, with remarkably high capacities of 2.80 mmol/g at 1 kPa and 3.37 mmol/g at 5 kPa for C3H8, as well as 2.93 mmol/g at 10 kPa for C2H6. Its IAST selectivities of C3H8/CH4 and C2H6/CH4 reached 274 and 29, respectively. The complete separation of CH4/C2H6/C3H8 ternary mixture on breakthrough experiment demonstrated the great potential on recovery of C2H6 and C3H8 from natural gas through a Ni(TMBDC)(DABCO)0.5 packed column.

A Stable Pillared-layer Metal-organic Framework for Recovery of C_2H_6 and C_3H_8 from Natural Gas

Yufang Wu,[a] Zewei Liu,[a] Xun Wang,*[a] Zhong Li,*[a,b]

[a] *School of Chemistry and Chemical Engineering, South China University of Technology, Guangzhou, 510640, China; E-mail: cezhli@scut.edu.cn*

[b]*State Key Lab of Subtropical Building Science of China, South China University of Technology, Guangzhou 510640, PR China*

Abstract: Separation and recovery of C_2H_6 and C_3H_8 from natural gas is a potentially economical but challenging subject in the petroleum industry. In this work, we report a stable pillared-layer microporous MOF, Ni(TMBDC)$(DABCO)_{0.5}$ for the separation of C_2H_6 and C_3H_8 from natural gas. Ni(TMBDC)$(DABCO)_{0.5}$ remained intact structure after exposure to humid air with RH = 100% for days. Derived from the combination of dense and accessible methyl group and methylene group in the channel, Ni(TMBDC)$(DABCO)_{0.5}$ exhibited strong affinity toward C_3H_8 and C_2H_6, with remarkably high capacities of 2.80 mmol/g at 1 kPa and 3.37 mmol/g at 5 kPa for C_3H_8, as well as 2.93 mmol/g at 10 kPa for C_2H_6. Its IAST selectivities of C_3H_8/CH_4 and C_2H_6/CH_4 reached 274 and 29, respectively. The complete separation of $CH_4/C_2H_6/C_3H_8$ternary mixture on breakthrough experiment demonstrated the great potential on recovery of C_2H_6 and C_3H_8 from natural gas through a Ni(TMBDC)$(DABCO)_{0.5}$ packed column.

Key words: Metal-organic framework, light hydrocarbons, natural gas, separation, stability

Introduction

Natural gas (NG), as a promising clean energy, has been widely used with an increasing trend in recent years.[1] Natural gas consists primarily of methane, including location-dependent ratio of 12 ~ 39% of other

heavier light hydrocarbons, such as ethane, propane, n-butane, etc.[2,3] Among these light hydrocarbons, C_2H_6 and C_3H_8 are of great value in the petrochemical industry. C_2H_6 is the most important raw material for the ethylene production which serves as the main component of the polyethylene, polyvinyl chloride and other polymer. C_3H_6 is also the basic feedstock for the propylene and polypropylene production.[3,4] Direct combustion of NG for heat supply without recovery of C_2H_6 and C_2H_8 would cause an enormous waste of these ethane (C2) and propane (C3) resources. Therefore, in order to fully utilize these hydrocarbons, it is essential to recover the ethane (C2) and propane (C3) from the natural gas for the high-purity alkene production. Although the cryogenic distillation, which is based on the small differences in boiling point of each component, may be used for the separation of C1/C2/C3, it is an energy-intensive separation technology.[3,5] Adsorptive separation is considered as one of the most promising techniques because of its low energy consumption and high separation efficiency.[1,6,7]

In adsorption technology, the adsorbent with excellent separation properties is the core.[7] Therefore, considerable efforts have been made to develop porous materials with high adsorption capacity and selectivity for separation of C1/C2/C3. Traditional porous materials, such as zeolites, carbonaceous materials, are employed to separate the C1/C2/C3 mixtures but most of them exhibited either low capacity or low selectivity for these hydrocarbons.[8,9] In recent years, metal-organic frameworks (MOFs), comprised of metal ions/clusters and organic linkers, has emerged and the diversity of the organic/inorganic linkers and exquisite control over pore aperture size promise MOFs great potential in the areas of gas storage,[10]catalysis,[11,12]sensing,[13,14] gas separations.[16-27]

Since the concentrations of ethane and propane are about 5% and 10% in natural gas respectively,[2] a MOF material with high gas capacity under low pressure area (5 kPa ~ 10 kPa) is highly demanded to address the issue of separation of C1/C2/C3. As a benchmark material for hydrocarbon separations, MOF-74(Co) was reported to adsorb 3 mmol/g propane at 5 kPa and 3.1 mmol/g ethane at 10 kPa, while it was humid unstable.[28,29] In addition, the Gly@HKUST-1 exhibited 4.22 mmol/g propane at 5 kPa and 1.19 mmol/g ethane at 10 kPa.[26] However, most of other MOFs reported for separation of C1/C2/C3 exhibited low adsorption capacity at low pressure region.[26-27, 36-38] In order to improve the C2/C3 low-pressure adsorption ability, a microporous MOF material with pore size slightly larger than molecule sizes of propane and ethane is required, which may lead to the enhancement of the interaction between framework and propane/ethane molecule. A pillared-layer MOF, Ni(TMBDC)$(DABCO)_{0.5}$[30], was found to show strong affinity towards C_2H_6 at low pressure area. In the structure of this material, the 2D-layer is connected by nickel paddle-wheels and 2,3,5,6-tetramethylterephthalic acid (TMBDC) and bridged by 1,4-Diazabicyclo[2.2.2]octane (DABCO) to produce a 3D network with the topology of pcu . The pore size of Ni(TMBDC)$(DABCO)_{0.5}$ is 0.59 nm, which is slightly larger than molecular sizes of propane (0.50 nm) and ethane (0.44 nm). Therefore, Ni(TMBDC)$(DABCO)_{0.5}$ would be a promising MOF material for the separation of C1/C2/C3.

Herein, we reported the synthesis of Ni(TMBDC)$(DABCO)_{0.5}$and its performance of separating light hydrocarbons for the recovery of C_3H_8 and C_2H_6 from natural gas. The stability of the material was estimated by TG analysis and PXRD characterization. The CH_4, C_2H_6 and C_3H_8 adsorption isotherms on Ni(TMBDC)$(DABCO)_{0.5}$ were measured and the separation performance of C1/C2/C3 ternary mixture was further evaluated by breakthrough experiment. The selectivity of C_2H_6/CH_4 and C_3H_8/CH_4 were predicted by ideal adsorbed solution theory (IAST) model. In addition, molecule simulation was applied to investigate the adsorption mechanism of these light hydrocarbons in the pores of Ni(TMBDC)$(DABCO)_{0.5}$.

Experimental

Materials

All chemical reagents were purchased from commercial sources (J&K Chemical, Aladdin, Macklin, et.al.) and used without further purifications. 2,3,5,6-Tetramethylterephthalic acid (TMBDC) was synthesized based on a reported procedure in the literature.[30,31]

Synthesis of Ni(TMBDC)$(DABCO)_{0.5}$

The $Ni(TMBDC)(DABCO)_{0.5}$ was synthesized according to the reported procedure[30]. Typically, in a 20 mL vial, $Ni(NO_3)_2{\cdot}6H_2O$ (0.093g, 0.32 mmol), DABCO (0.018g, 0.16 mmol), TMBDC (0.067 g, 0.03 mmol) were mixed in 8 mL DMF and then 1 drop of HNO_3 was added, followed by sonication for 5 min. The resulting green solution was heated at 120 for 48 h to afford the green crystals. The crystals were collected by filtration and washed in DMF to remove the excess reactants and then soaked into ethanol for 2 days. The obtained $Ni(TMBDC)(DABCO)_{0.5}$ was kept in ethanol before further experiments.

Characterizations

The N_2 adsorption-desorption isotherms were measured on Micrometrics ASAP 2460 at 77 K using a liquid N_2 bath. The BET surface area was calculated using the Brunauer-Emmett-Teller equation in the range $P/P_0 = 0.05 - 0.35$ and the pore size distribution was calculated by DFT method based on the N_2 adsorption amount at the pressure of $P/P_0 = 0.95$. The sample was filtered using a Buchner funnel and degassed at 120 for 6 h before each analysis.

Powder X-ray diffraction (PXRD) was performed on the Bruker AXS D8 Advance using Cu Kα (λ=1.5406 Å) radiation at 5° – 40°. TGA curve was measured on NETZSCH STA 449F3 Simultaneous Thermal Analyzer (NETZSCH, Germany) at temperature range of 30 °C to 700 °C with 10 °C/min heating rate under N_2 atmosphere.

Adsorption isotherms measurement

The single component adsorption isotherms of CH_4, C_2H_6 and C_3H_8 were collected on 3Flex Surface Characterization Analyzer (Micromeritics, USA) at 288 K, 298 K and 308 K. Prior to each measurement, the ethanol-soaked sample was filtered and then degassed at 120 under vacuum for 6 h.

Stability test

To investigate the stability of $Ni(TMBDC)(DABCO)_{0.5}$ in varied solution or under humidity conditions, the ethanol soaked sample was filtered and dried in the air firstly and then immersed into varied solution (acetone, hexane, dichloromethane) or exposed to humid air with RH =100% and RH = 55%, respectively. After 4 days, the samples were collected by filtration and characterized by PXRD technique.

Breakthrough experiments

The breakthrough curves of gas mixture $CH_4/C_2H_6/C_3H_8$(85:10:5, v/v/v) were measured on a self-assembly experimental apparatus (ESI). The carrier gas was N_2 with flow rate of 45 mL/min and the flow rate of $CH_4/C_2H_6/C_3H_8$mixture gas was controlled at 5 mL/min by a mass flow controller (FMA-A200, America). The composition of exit gas stream from the adsorption column was determined on-line on a gas chromatography apparatus (GC-9560, Shanghai Huaai), equipped with a 2 m long Al_2O_3-packed column with an FID detector. Typically, about 300 mg dry sample was packed into a stainless steel column with inner dimension of Φ3 × 275 mm. The six-way valve was used to collect and send the sample gas with constant amount into the GC automatically every 90 seconds. For the cycling tests, the sample packed column was regenerated by purging N_2 flow (30 mL/min) at 100 °C for 30 min. After that the gas flow was switched to $CH_4/C_2H_6/C_3H_8$mixture for the next cycle.

Simulation details

Adsorption properties of pure CH_4, C_2H_6 and C_3H_8 on $Ni(TMBDC)(DABCO)_{0.5}$ were simulated by Grand Canonical Monte Carlo (GCMC) method. All GCMC simulations were carried out by the Sorption modules in Materials Studio (Version 2017 R2). In this study, the universal force field (UFF) was adopted. The Ewald summation method was used to calculate the electrostatic energy and the atom based method was applied to describe the van der Waals interaction.

Results and discussion

Characterization of samples

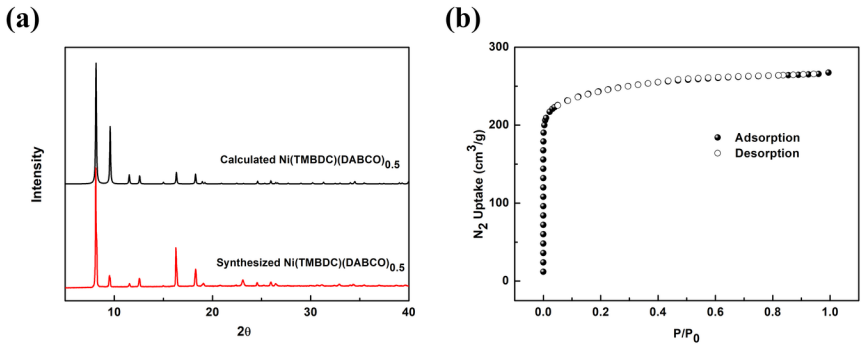

Figure 1 (a) PXRD patterns of fresh and calculated Ni(TMBDC)(DABCO)$_{0.5}$; (b) N_2adsorption-desorption isotherms of Ni(TMBDC)(DABCO)$_{0.5}$at 77 K

Figure 1(a) presents the comparison between the calculated and experimental PXRD patterns of the sample Ni(TMBDC)(DABCO)$_{0.5}$. It can be observed that the PXRD pattern of the synthesized Ni(TMBDC)(DABCO)$_{0.5}$ shows two obvious characteristic peaks at 8.1° and 9.5°, which are in good agreement with the calculated PXRD pattern, suggesting the successful synthesis of the Ni(TMBDC)(DABCO)$_{0.5}$.

To assess the permanent porosity of the Ni(TMBDC)(DABCO)$_{0.5}$, N_2adsorption-desorption isotherms were measured at 77 K. As shown in Figure 1(b), the N_2 adsorption-desorption isotherms of Ni(TMBDC)(DABCO)$_{0.5}$ exhibits a characteristic type-I isotherm with steeply increasing N_2 adsorption capacity at relatively low pressures and a maximum N_2 uptake of 267 cm^3/g at $P/P_0 = 1$ was achieved, indicating its microporosity. Derived from the N_2 isotherms, the BET surface area and total pore volume of Ni(TMBDC)(DABCO)$_{0.5}$ are 940 m^2/g and 0.41 cm^3/g, respectively. The pore size of Ni(TMBDC)(DABCO)$_{0.5}$ is uniformly 0.5 nm, as shown in Figure S2, which is amenable to kinetic diameters of C_3H_8 and C_2H_6, implying the great potential on separation of C3/C2/C1 mixture.

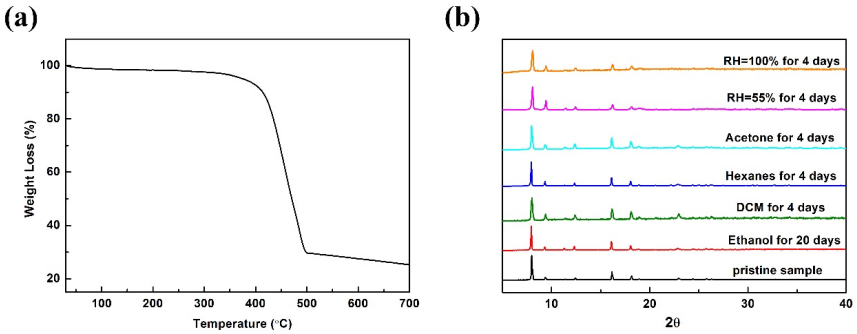

Figure 2 (a) TGA curve of Ni(TMBDC)(DABCO)$_{0.5}$; (b) PXRD patterns of Ni(TMBDC)(DABCO)$_{0.5}$ before and after various treatment.

TGA data were collected for the evaluation of the thermal stability of the Ni(TMBDC)(DABCO)$_{0.5}$. Figure 2(a) presents the TGA curve of Ni(TMBDC)(DABCO)$_{0.5}$. It is noticed that the TGA curve showed a negligible weight loss (˜5%) before 400 ºC which was attributed to the removal of guest molecules such as H_2O molecule. After 400 °C, a great weight loss (˜68%) occurred due to the decomposition of the framework structure. It suggests that the Ni(TMBDC)(DABCO)$_{0.5}$ is thermally stable until 400 ºC.

We also examined the solvent stability and water vapor stability of the Ni(TMBDC)(DABCO)$_{0.5}$. Figure 2(b) shows the PXRD patterns of Ni(TMBDC)(DABCO)$_{0.5}$ before and after soaking in various solvents or

exposure to humid air for several days. It is visible that the Ni(TMBDC)$(DABCO)_{0.5}$ retained the structural integrity after soaking separately in acetone, DCM, Hexanes for 4 days and ethanol for 20 days, demonstrating excellent stability in these organic solvents. Furthermore, the water vapor stability was tested by exposing the Ni(TMBDC)$(DABCO)_{0.5}$ to humid air with 55% and 100% humidity for 4 days. The PXRD patterns of Ni(TMBDC)$(DABCO)_{0.5}$ after exposure to humid air are similar to that of the fresh material, suggesting its excellent humid stability. The water vapor stability could be attributed to the hydrophobicity of the channel of Ni(TMBDC)$(DABCO)_{0.5}$, which is caused by the methyl group on the TMBDC ligand and the methylene group on the DABCO ligand.

CH_4, $C_2H_6$and C_3H_8 isotherms and C_2H_6/CH_4, C_3H_8/CH_4 selectivity of the sample

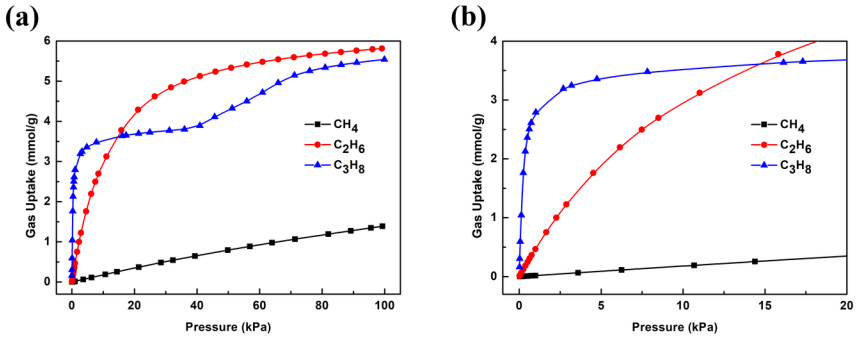

Figure 3 CH_4, C_2H_6 and C_3H_8 adsorption isotherms of Ni(TMBDC)$(DABCO)_{0.5}$ at 298 K in the pressure region of (a) 0 ˜100 kPa and (b) 0 ˜ 20 kPa

Figure 3 presents the CH_4, C_2H_6 and C_3H_8 adsorption isotherms of Ni(TMBDC)$(DABCO)_{0.5}$ at 298 K. The C_3H_8 and C_2H_6 uptakes on Ni(TMBDC)$(DABCO)_{0.5}$ are much higher than CH_4, reaching as high as 5.54 mmol/g and 5.81 mmol/g at 100 kPa, respectively. As shown in Figure 3(b), at low pressure region of 0 ˜ 15 kPa, the C_3H_8isotherm exhibits a steeply increasing trend in C_3H_8 adsorption capacity and the uptake of each gas in Ni(TMBDC)$(DABCO)_{0.5}$ decreased in the order of $C_3H_8 > C_2H_6 > CH_4$. It implies that the interaction between C_3H_8 and Ni(TMBDC)$(DABCO)_{0.5}$ is the strongest, that of C_2H_6 is in the second place, and that of CH_4 is the weakest, which is mainly determined by the property of CH_4, $C_2H_6$and C_3H_8, especially molecule polarizabilities. The polarizability is considered as an important intrinsic property of a molecule that reflects the ability to generate instantaneous dipole related to Van der Waals interactions within the molecule, which dominate the interactions between the molecule and an adsorbent.[32, 40] The polarizabilities of C_3H_8, C_2H_6 and CH_4 are 62.9–63.7×10^{25}, 44.3–44.7×10^{25}, 25.93×10^{25} cm^{-3}, respectively.[16] Therefore, C_3H_8 and C_2H_6 would likely exhibited stronger interaction towards the surface of Ni(TMBDC)$(DABCO)_{0.5}$. The strong interaction is also evidenced by the isosteric heat (Q_{st}). As presented in Figure S5, the Q_{st} values of C_3H_8 and C_2H_6 reached 59 kJ/mol and 36 kJ/mol at 0.5 kPa, respectively, while that of CH_4 is 14 kJ/mol, demonstrating strong interaction of $C_3H_8$and C_2H_6 within Ni(TMBDC)$(DABCO)_{0.5}$. It is noticed that, at the pressure region of 15 ˜ 100 kPa, the uptake of C_3H_8 is lower than C_2H_6. This should be attributed that the molecular kinetic diameter of C_3H_8 (4.3 ˜ 5.1 Å) is larger than that of C_2H_6 (4.4 Å), thus less C_3H_8 molecules could be accommodated in the limited pore volume of Ni(TMBDC)$(DABCO)_{0.5}$ compared to C_2H_6.

It is worth to mention that the Ni(TMBDC)$(DABCO)_{0.5}$adsorbed C_3H_8 with a gate opening behavior at three temperatures as shown in Figure S6. The gate-opening pressure (P_{go}) for C_3H_8 decreased from 68 kPa at 308 K to 23 kPa at 288 K. Such breathing behavior on hydrocarbon adsorption were observed on ELM-11,[33]Cu$(dhbc)_2$(4,4'-bipy),[34]USTA-300,[23] ZIF-7[35], etc. The gate-opening behavior of Ni(TMBDC)$(DABCO)_{0.5}$ is considered to be induced by the adsorption of C_3H_8 molecule.[34]The framework of the material had strong interaction with the adsorbed C_3H_8 molecule due to the methyl group and me-

thylene group in the channel, leading to a structural transition after the first saturated adsorption capacity of C_3H_8 was obtained. As the temperature decreased, the thermal motion of C_3H_8molecule slowed down so that the C_3H_8molecule could be adsorbed more easily on the Ni(TMBDC)$(DABCO)_{0.5}$, thereby leading to lower gate-opening pressure (P_{go}).[34]

Particularly, since the concentrations of ethane and propane are relatively low in natural gas, the adsorption ability of ethane and propane at low pressure region (0 ˜ 20 kPa) is basically important for the separation performance of C1/C2/C3. For comparison, Table 1 summarizes the low-pressure adsorption capacity of some materials for C_2H_6 and C_3H_8. It is clearly visible that the C3 and C2 uptakes in Ni(TMBDC)$(DABCO)_{0.5}$ at low pressure region are comparable with those of MgMOF-74 and 0.3Gly@HKUST-1, and higher than other reported materials, such as MOFs and porous carbon materials, indicating a great potential of Ni(TMBDC)$(DABCO)_{0.5}$ for separating C1/C2/C3.

Table 1 Comparison of C_2H_6/C_3H_8adsorption capacity and C_2H_6/CH_4 and C_3H_8/CH_4 selectivities of some reported materials

Materials
Ni(TMBDC)$(DABCO)_{0.5}$
MgMOF-74[a]
Fe_2(dobdc) [a]
MFM-202a[b]
UTSA-35a[c]
FIR-7a-ht[d]
ZnSDB
0.3Gly@HKUST-1[d]
A-AC-4[d]

[a] Data was collected at 318 K and 1 bar; [b] Data was collected at 293 K and 1 bar; [c] Data was collected at 296 K and 1 bar

The ideal adsorbed solution theory model (IAST) was applied to predict the selectivity of binary mixtures of C_2H_6/CH_4 and C_3H_8/CH_4 on Ni(TMBDC)$(DABCO)_{0.5}$, respectively. Firstly, dual-site Langmuir-Freundlich (DSLF) model was used to fit the single component adsorption isotherms of $CH_4/C_2H_6/C_3H_8$at 298 K. [33] The fitting parameters and correlation coefficients R^2 from DSLF model are listed in Table S2. The R^2 of the fitting curves for CH_4, C_2H_6 and C_3H_8 adsorption isotherms are up to 0.999, indicating the well description of the CH_4, C_2H_6 and C_3H_8 adsorption behaviors on Ni(TMBDC)$(DABCO)_{0.5}$ by DSLF model.

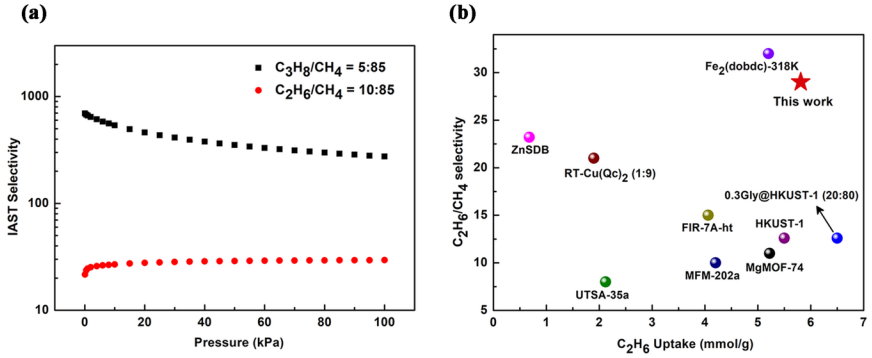

Figure 4 (a) IAST selectivity of C_2H_6/CH_4 (10:85, v/v) and /C_3H_8/CH_4 (5:85, v/v) binary mixtures on Ni(TMBDC)$(DABCO)_{0.5}$ at 298 K; (b) Comparison of selectivity for Ni(TMBDC)$(DABCO)_{0.5}$and other

reported MOFs

Figure 4(a) shows the IAST selectivities of Ni(TMBDC)$(DABCO)_{0.5}$ at 298 K for the C_2H_6/CH_4 (10:85, v/v) and C_3H_8/CH_4 (85:5, v/v) binary mixtures. The C_2H_6/CH_4 selectivity reached as high as 29 at 298 K and 100 kPa, and its C_3H_8/CH_4 selectivity exhibited a descending trend in the range of 0 ~ 100 kPa and reached as high as 274, which are higher than most of the materials reported to date, as shown in Table 1. Moreover, Figure 4(b) summarizes C_2H_6/CH_4 selectivities of Ni(TMBDC)$(DABCO)_{0.5}$ and other MOFs materials. It is shown that Ni(TMBDC)$(DABCO)_{0.5}$ exhibits not only high C_2H_6 capacity but also C_2H_6/CH_4 selectivity compared to other MOFs, which could potentially address the trade-off between adsorption capacity and selectivity.

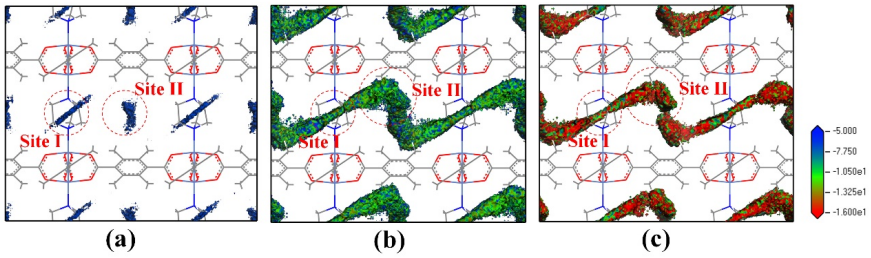

Figure 5 Simulated adsorption density distribution colored by adsorption potential of (a) CH_4, (b) C_2H_6 and (c) C_3H_8 in Ni(TMBDC)$(DABCO)_{0.5}$ at 1 kPa

To further understand the adsorption mechanism of CH_4, C_2H_6 and C_3H_8 in Ni(TMBDC)$(DABCO)_{0.5}$, the GCMC was applied to examine the adsorption density distribution of the three gases in the adsorbent. As illustrated in Figure 5, the CH_4, C_2H_6 and C_3H_8 were adsorbed on two sites in the framework of Ni(TMBDC)$(DABCO)_{0.5}$, which are termed as Site I and Site II. The gases adsorbed on Site I was mainly influenced by the methylene group from DABCO pillar, while those adsorbed on Site II was affected synergistically by the methyl group from TMBDC ligand and the methylene group from the adjacent DABCO pillar. That is to say, strong interaction was formed on CH_4, C_2H_6 and C_3H_8 molecule owing to the presence of methyl and methylene group, and thus these hydrocarbon molecules were more preferentially adsorbed on the Site II and Site I.

In addition, it shows that the adsorption potentials of these alkanes in the Ni(TMBDC)$(DABCO)_{0.5}$ follow the order: $C_3H_8 > C_2H_6 > CH_4$, which is consistent with the order of the adsorption capacity at low pressure region. This phenomenon further confirmed that the framework of Ni(TMBDC)$(DABCO)_{0.5}$ showed stronger affinity toward C_3H_8 than C_2H_6 and CH_4, which was attributed to the existence of both methyl groups and methylene groups in the channel.

Figure 6 Breakthrough curves of $CH_4/C_2H_6/C_3H_8$(85:10:5, v/v/v) ternary mixtures through Ni(TMBDC)$(DABCO)_{0.5}$ packed column

To evaluate the dynamic separation performance of the sample for $CH_4/C_2H_6/C_3H_8$mixture, breakthrough experiments at 298 K were performed, in which the stimulated industrial gas mixture of $CH_4/C_2H_6/C_3H_8$(85:10:5, v/v/v) was applied. Figure 6 presents the breakthrough curves of ternary mixtures $CH_4/C_2H_6/C_3H_8$(85:10:5, v/v/v) through the packed column with Ni(TMBDC)$(DABCO)_{0.5}$. It demonstrates that these three gases were completely separated with the breakthrough time of 80 min for C_3H_8, 24 min for C_2H_6, and 4 min for CH_4. In addition, the recyclability of Ni(TMBDC)$(DABCO)_{0.5}$was also examined. Figure S7 presents the breakthrough curves of three adsorption-desorption cycles on Ni(TMBDC)$(DABCO)_{0.5}$. It shows that the breakthrough curves of these ternary mixtures almost overlap, indicating excellent recycling performance of Ni(TMBDC)$(DABCO)_{0.5}$. These great separation property

and recyclability of the Ni(TMBDC)$(DABCO)_{0.5}$ would make it a great candidate for challenging separation of $CH_4/C_2H_6/C_3H_8$mixture or recovering low content of C_2H_6 and C_3H_8 from natural gas.

Conclusion

In summary, we synthesized a microporous metal-organic framework, Ni(TMBDC)$(DABCO)_{0.5}$ and investigated its separation performance for recovery low content of C_2H_6 and C_3H_8 from natural gas. The as-synthesized Ni(TMBDC)$(DABCO)_{0.5}$ showed good thermal stability, solvent stability and humid stability under RH = 100%. Due to the strong interaction between the framework and the guest molecule, the gate opening behavior of C_3H_8adsorption on the Ni(TMBDC)$(DABCO)_{0.5}$ was observed and the remarkably high capacities of 2.80 mmol/g at 1 kPa and 3.37 mmol/g at 5 kPa were obtained. The IAST-predicted selectivity of Ni(TMBDC)$(DABCO)_{0.5}$ reached as high as 274 for C_3H_8/CH_4 (5:85, v/v) and 29 for C_2H_6/CH_4 (10:85). The breakthrough experiment revealed that simulated gas mixture of C1/C2/C3 was well separated on the Ni(TMBDC)$(DABCO)_{0.5}$material. The molecular simulation further confirmed the methylene groups and methyl groups played a crucial role on C_3H_8 and C_2H_6 adsorption. This work unveils that the Ni(TMBDC)$(DABCO)_{0.5}$ with good stability and unique pore environment is a promising material for recovering ethane and propane from natural gas or other hydrocarbon separation. Looking ahead, the shaping of Ni(TMBDC)$(DABCO)_{0.5}$, for example, from powder to spherical adsorbents with excellent mechanical strength, is undergoing in our group, which is necessary before practical applications.

Acknowledgements

The authors gratefully acknowledge the National Natural Science Foundation of China (No. 21436005, No. 21978099), the Research Foundation of State Key Lab of Subtropical Building Science of China (2018ZC08) and the Guangdong Province Science and Technology Project (No. 2016A020221006) for the support of this work.

References

[1] D. S. Sholl, R. P. Lively. Seven chemical separations to change the world. *Nature* ., 2016, **532** , 435-437.

[2] J. Shen, A. Dailly, M. Beckner. Natural gas sorption evaluation on microporous materials. *Micropor. Mesopor. Mat* ., 2016,**235** , 170-177.

[3] S. Mater, L. F. Hatch. Chemistry of Petrochemical Processes 2nd edition; Gulf Publishing Company: 2001

[4] R. B. Eldridge. Olefin/paraffin separation technology: a review,*Ind. Eng. Chem. Res* ., 1993, **32** , 2208-2212.

[5] T. Ren, M. Patel, K. Blok. Olefins from conventional and heavy feedstocks: Energy use in steam cracking and alternative processes.*Energy* ., 2006, **31** (4), 425-451.

[6] D. M. Ruthven, Principles of adsorption and adsorption process. John Wiley $ Sons: 1984

[7] R. T. Yang, Adsorbents: fundamentals and applications. John Wiley & Sons: 2003

[8] S. Hosseinpour, S. Fatemi, Y. Mortazavi, et al. Performance of CaX zeolite for separation of C_2H_6, C_2H_4, and CH_4 by adsorption process; Capacity, selectivity, and dynamic adsorption measurements. *Sep. Sci. Technol* ., 2010, **46** , 349-355.

[9] A.M. Avila, F. Yang, M. Shi, S.M. Kuznicki. Extraction of ethane from natural gas at high pressure by adsorption on Na-ETS-10.*Chem. Eng. Sci* ., 2011, **66** , 2991–2996.

[10] B. Li, Y. Cui, W. Zhou, G Qian, B. Chen. Emerging multifunctional metal–organic framework materials. *Adv. Mater.* , 2016, **28** , 8819-8860

[11] J. Y. Lee, O. K. Farha, J. Roberts, S. T. Nguyen, J. T. Hupp. Metal-organic frameworks as catalysts. *Chem. Soc. Rev.* , 2009,**38** , 1450-1459

[12] H. Furukawa, K. E. Cordova, M. O'Keeffe, O. M. Yaghi. The chemistry and applications of metal-organic frameworks. *Science.* , 2013, 341, 1230444-(1 - 12)

[13] Z. Hu, B. J. Deibert, J. Li. Luminescent metal–organic frameworks for chemical sensing and explosive detection. *Chem. Soc. Rev.* , 2014, **43** , 5815-5840

[14] L. E. Kreno, K. Leong, O. K. Farha, J. T. Hupp. Metal–organic framework materials as chemical sensors. *Chem. Rev.* , 2012,**112** , 1105-1125

[15] N. L. Rosi, J. Eckert, M. Eddaoudi, M. O'Keeffe, O. M. Yaghi. Hydrogen storage in microporous metal-organic frameworks.*Science* ., 2003, **300** , 1127-1129

[16] J. –R. Li, R. J. Kuppler, H. -C. Zhou. Selective gas adsorption and separation in metal–organic frameworks. *Chem. Soc. Rev.* , 2009, **38** , 1477-1504

[17] R. –B. Lin, S. Xiang, H. Xing, W. Zhou, B. Chen. Exploration of porous metal–organic frameworks for gas separation and purification.*Coord. Chem. Rev.* , 2019, **378** , 87-103

[18] Z. Zhou, C. Ma, J. Xiao, Q. Xia, Z. Li. A novel bimetallic MIL-101(Cr, Mg) with high CO_2 adsorption capacity and CO_2/N_2 selectivity. *Chem. Eng. Sci.* , 2016, **147,** 109-117

[19] Z. Zhang, Z. -Z. Yao, S. Xiang, B, Chen. Perspective of microporous metal–organic frameworks for CO_2 capture and separation. *Energy. Environ. Sci.* , 2014, 7, 2868-2899

[20] W. Huang, X. Zhou, Q. Xia, J. Peng, H. Wang, Z. Li. Preparation and adsorption performance of GrO@Cu-BTC for separation of CO_2/CH_4. *Ind. Eng. Chem. Res.* , 2014, **53** , 11176-11184

[21] M. K. Taylor, T. Runčevski, J. Oktawiec, J. E. Bachman, J. R. Long. Near-perfect CO_2/CH_4 selectivity achieved through reversible guest templating in the flexible metal–organic framework Co(bdp). *J. Am. Chem. Soc.* , 2018,**140** , 10324-10331

[22] Y. Ye, Z. Ma, R. -B. Lin, R. Krishna, W. Zhou, B. Chen. Pore Space partition within a metal–organic framework for highly efficient C_2H_2/CO_2 separation.*J. Am. Chem. Soc.* , 2019, **141** , 4130-4136

[23] R. –B. Lin, L. Li, H. Wu, H. Arman, B. Li, W. Zhou, B. Chen. Optimized separation of acetylene from carbon dioxide and ethylene in a microporous material. *J. Am. Chem. Soc.* , 2017, **139** , 8022-8028

[24] P. -Q. Liao, W. -X. Zhang, J. -P. Zhang, X. -M. Chen. Efficient purification of ethene by an ethane-trapping metal-organic framework.*Nat. Commun.* , 2015, **6** , 8697-8705[25] W. Liang, F. Xu, X. Zhou, J. Xiao, Z. Li. Ethane selective adsorbent Ni(bdc)$(ted)_{0.5}$ with high uptake and its significance in adsorption separation of ethane and ethylene. *Chem. Eng. Sci.* , 2016, **148** , 275-281

[26] Y. Wu, Y. Sun, J. Xiao, X. Wang, Zhong Li. Glycine-modified HKUST-1 with simultaneously enhanced moisture stability and improved adsorption for light hydrocarbons separation. *ACS Sustainable Chem. Eng.* , 2019, **7** , 1557-1563

[27] S. Gao, C. G. Morris, Z. Lu, Y .Yan, K. M. Thomas, S. Yang, M. Schroder. Selective hysteretic sorption of light hydrocarbons in a flexible metal-organic framework material. *Chem. Mater.* , 2016,**28** , 2331-2340

[28] Y. He, R. Krishna, B. Chen. Metal–organic frameworks with potential for energy-efficient adsorptive separation of light hydrocarbons. *Energy Environ. Sci.* , 2012, **5** , 9107-9120

[29] E. D. Bloch, W. L. Queen, R. Krishna, J. M. Zadrozny, C. M. Brown, J. R. Long. Hydrocarbon separations in a metal-organic framework with open iron(II) coordination sites. *Science.* , 2012,**335** , 1606-1610

[30] X. Wang, Z. Niu, A. M. Al-Enizi, L. Wojtas, Y. -S. Chen, Z. Li, S. Ma. Pore environment engineering in metal-organic frameworks for efficient ethane/ethylene separation. *J. Mater. Chem. A.* , 2019,**7** , 13585-13590

[31] A. Hijazi, S. Floquet, J. Marrot, J. Fize, V. Artero. Tuning the electrocatalytic hydrogen evolution reaction promoted by $[Mo_2O_2S_2]^{-}$based molybdenum cycles in aqueous medium. *Dalton Trans.* , 2013,**42** , 4848-4858

[32] W. Liang, H. Xiao, D. Lv, J. Xiao, Z. Li. Novel asphalt-based carbon adsorbents with super-high adsorption capacity and excellent selectivity for separation for light hydrocarbons. *Sep. Purif. Technol.* , 2018, **190** , 60-67

[33] L. Li, R. Krishna, Y. Wang, X. Wang, J. Yang, J. Li. Flexible metal–organic frameworks with discriminatory gate opening effect for the separation of acetylene from ethylene/acetylene mixtures. *Eur. J. Inorg. Chem.* , **2016** , 4457–4462

[34] Li L., Krishna R., Wang Y., J. Li. Exploiting the gate opening effect in a flexible MOF for selective adsorption of propyne from C1/C2/C3 hydrocarbons. *Journal of Materials Chemistry A* . 2016,**4** (3), 751-755.

[35] C. Gücüyener, J. Bergh, J. Gascon, F. Kapteijn, Ethane/ethene separation turned on its Head: selective ethane adsorption on the metal-organic framework ZIF-7 through a gate-opening mechanism. *J. Am. Chem. Soc.* , 2010, **132** , 17704–17706

[36] Y. He, Z. Zhang, S. Xiang, B. Chen. A robust doubly interpenetrated metal-organic framework constructed from a novel aromatic tricarboxylate for highly selective separation of small hydrocarbons. *Chem. Commun* ., 2012, **48** , 6493-6495.

[37] He Y. P., Tan Y. X., Zhang J. Tuning a layer to a pillared-layer metal-organic framework for adsorption and separation of light hydrocarbons. *Chem. Commun* ., 2013, **49** , 11323-11325.

[38] F. -S. Tang, R. -B. Lin, R. -G. Lin, B. Chen. Separation of C2 hydrocarbons from methane in a microporous metal-organic framework.*J. Solid. State. Chem* ., 2018, **258** , 346-350.

[40] S. Du, Y. Wu, X. Wang, Q. Xia, J. Xiao, Z. Li. Facile synthesis of ultramicroporous carbon adsorbents with ultrahigh CH4 uptake by in situ ionic activation. *AIChE J.* 2020; e16231.